Materials Physics and Mechanics 17 (2013) 47-58 Received: May 10, 2013

SYNTHESIS, CHARACTERIZATION AND SURFACE DEFORMATION STUDY OF NANOCRYSTALLINE Ag_2Se THIN FILMS

U.M. Chougale[1], S.H. Han[2], M.C. Rath[3], V.J. Fulari[1*]

[1]Holography and Materials Research Laboratory, Department of Physics, Shivaji University, Kolhapur-416 004, India

[2]Department of Chemistry, Hanyang University, Seoul, South Korea.

[3]Radiation and Photochemistry Division, BARC, Mumbai, India

*e-mail: vijayfulari@gmail.com

Abstract. Herein we report electrochemical synthesis of the silver selenide (Ag_2Se) thin films using simple and economical electrodeposition method in potentiostatic mode at room temperature (~ 27 ^oC). Growth of rhombohedral Ag_2Se nanocrystals having size 63 to 75 nm were observed in (201) direction. Band gap energy of Ag_2Se decreased from 1.3 eV to 1.1 eV and contact angle increases from 58 ^{o} to 74 ^{o} with increase in bath concentration from 3 to 5 mM. A possible mechanism for the growth and stress of compact granular Ag_2Se nanocrystals is discussed with DEHI technique. Compared with previous methods, present method shows simple and easiest way to synthesize nanosized Ag_2Se particles in one step.

1. Introduction

Silver selenide (Ag_2Se) belongs to I–VI semiconductor compound rarely found in the nature as mineral naumannite. Silver selenide (Ag_2Se) is a promising material for technological applications in various fields such as thermo-chromic material for non-linear optical devices, multipurpose ion-selective electrodes, infrared sensors, electrochemical storage cells, electrochemical potential memory devices, magnetic field sensing devices etc [1-3]. Silver selenide (β- Ag_2Se) is an important n-type semiconductor with a narrow band gap [4, 5]. Ag_2Se is a mixed ionic conductor with a transition from a low temperature orthorhombic phase (β- Ag_2Se) to a high-temperature super ionic conducting cubic phase (α- Ag_2Se) at 135 °C [6]. Its high temperature phase (α-Ag_2Se) is a super-ionic conductor used as solid electrolyte in photochargable batteries [7]. Its low temperature phase (β-Ag_2Se) has been widely exploited as a thermo-chromic material, as photo sensitizer in photographic films [8]. Nonstoichiometric Ag_2Se also shows giant magneto resistance comparable to the colossal magneto resistance observed in manganese perovskites [9, 10]. All the above properties of Ag_2Se are studied in bulk form and the physical properties of semiconducting material are size dependent. As semiconductor nanocrystals finding various applications in solar cells [11], light-emitting diodes [12, 13], thin-film transistors [14, 15] and biological imaging [16], the control over particle size and morphology became very much important from a fundamental and industrial point of view. In this direction synthesis of Ag_2Se with different methods has been carried out by various workers. Vacuum evaporated Ag_2Se thin films were used to study the phase transition temperature as a function of thickness [17]. Substitution deposition method [18], adsorption- reduction method [19], chemical bath deposition [20], reactive evaporation method [5], electrodeposition [21, 22] and solvo-thermal technique [23]

Ag (Fig. 1(a)), while reduction of Se^{4+} to Se occurs at -0.1 to -0.45 V (Fig. 1(b)). There are two anodic peaks on curve corresponding to the oxidation of Ag (at 0.8 V) and oxidation of Se^{2-} to Se^0 (at - 0.45 V) (Fig. 1(c)). Se^{2-} is formed during the reduction of H_2SeO_3 (at - 0.1 V). Oxidation of Se to Se^{4+} occurs at – 1.0 V. Cathodic peak at – 0.7 V is related with reduction of Se^{4+} to Se while reduction of Ag^+ occurs at + 0.4 V [26]. From Fig. 1(c) it is seen that the cathodic current increases - 0.2 V to - 0.4 V. Thus the deposition of Ag_2Se takes place at this particular reduction potential [27].

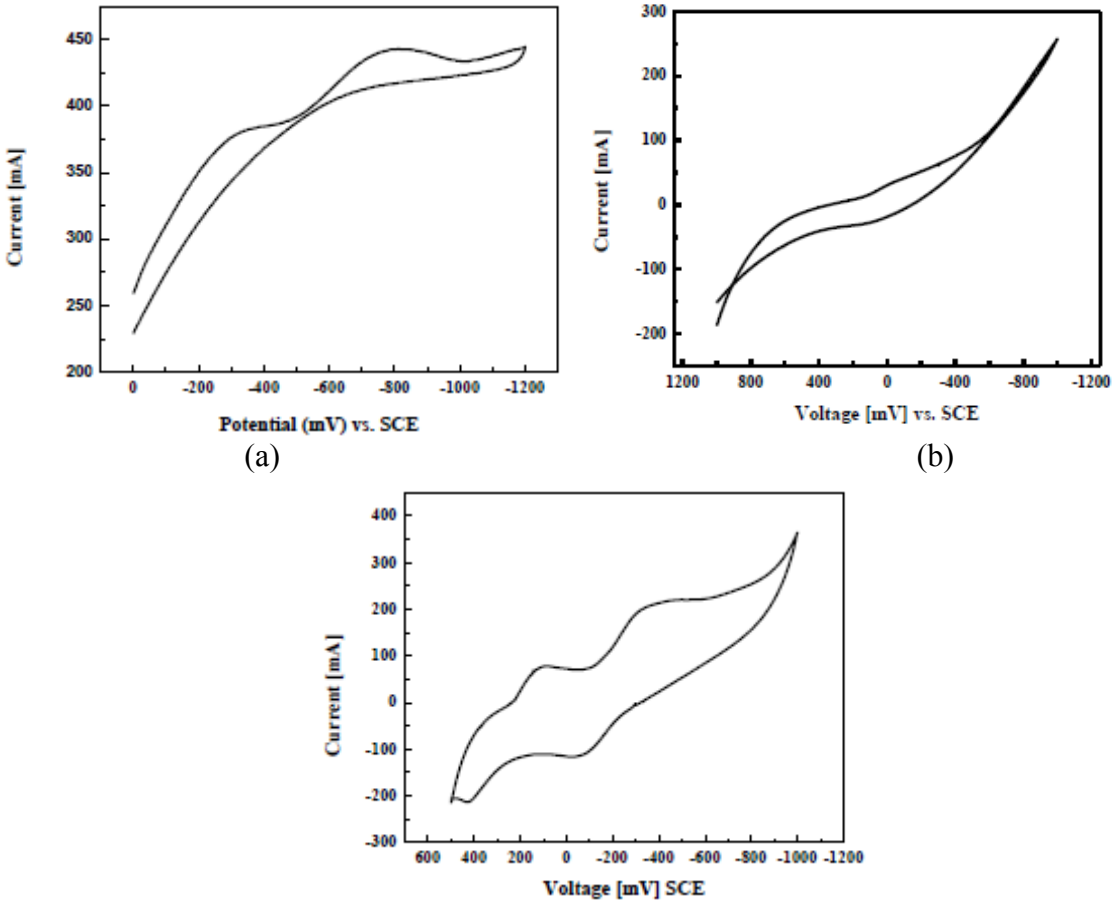

Fig. 1. Cyclic voltammogram for (a) 5 mM $AgNO_3$, (b) 5 mM SeO_2, (c) 5 mM ($AgNO_3$+SeO_2).

3.2. Reaction mechanism. The chemical reaction for the deposition of silver selenide films taking place in bath could be considered as below:
The aqueous solution of silver nitrate forms

$$AgNO_3 + H_2O \rightarrow Ag^+ + HNO_3 + OH^-, \quad (1a)$$

Selenium dioxide forms

$$SeO_2 + H_2O \rightarrow HSeO_3^- + H^+ . \quad (1b)$$

The final reaction takes place for the formation of Ag_2Se film:

$$2Ag^+ + HSeO_3^- + 5H^+ + 4e^- \rightarrow Ag_2Se + 3H_2O. \quad (2)$$

3.3. X-ray diffraction. Figure 2 shows X-ray diffraction patterns of three Ag_2Se thin film samples I, II and III for different bath concentration (A), (B) and (C) respectively

Table 2. Variation in particle size, contact angle and band gap energy of Ag_2Se thin films.

Sample		Particle size for (hkl) planes, nm		Contact Angle, degree		Band gap energy, eV	
	(112)	(121)	(201)	(221)	Mean		
A	55.90	62.45	62.40	72.88	63.41	58	1.31
B	56.40	66.27	66.46	86.05	68.80	63	1.20
C	90.19	62.46	62.40	85.83	75.22	74	1.13

3.4. Surface morphology. The microstructure of Ag_2Se thin films on to stainless steel substrate was analyzed by scanning electron microscope technique for samples I, II and III. From the micrographs (Fig. 3), it is seen that the Ag_2Se particles cluster into uniformly distributed grains over smooth homogenous background. Also grain size increases with increasing concentration. The growth of the nanostructures takes place through two steps namely nucleation followed by growth, in first step the Ag_2Se nuclei are formed due to the applied potential. These nuclei having high surface energy tend to aggregate by minimizing interfacial energy which tends to larger particle size. This suggests that increase in bath concentration favor both particle growth and aggregation. The well developed and matured Ag_2Se particle growth is observed as Van der Waals interaction between Ag_2Se leads to the self assembly and aggregation of Ag_2Se nanocrystals [31]. Different methods yield different morphologies of Ag_2Se thin films used in various applications. Single crystalline Ag_2Se nano wires and polycrystalline Ag_2Se tubes [32], nanofiber bundles [33], nano tubes [26], nano crystals [4, 23, 34] were synthesized. Reactive evaporation method yielded Ag_2Se nanocrystals having grain size 650 nm [23]. Though solvothermal method with single precursor yield nano crystals of Ag_2Se with grain size between 25 – 40 nm, the reaction temperature is 250 ^oC [34] and we are reporting facile room temperature synthesis of nanocrystalline Ag_2Se with grain size of the order 63 nm. This type of morphology will be useful in the surface area dependent application of semiconducting Ag_2Se nano crystals in photo-catalysis and solar cell.

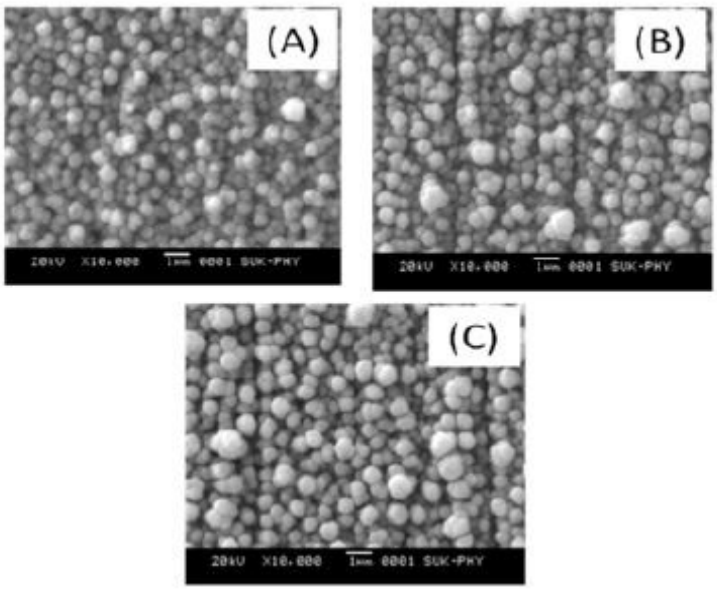

Fig. 3. Micrographs of Ag_2Se thin film for different bath concentrations.

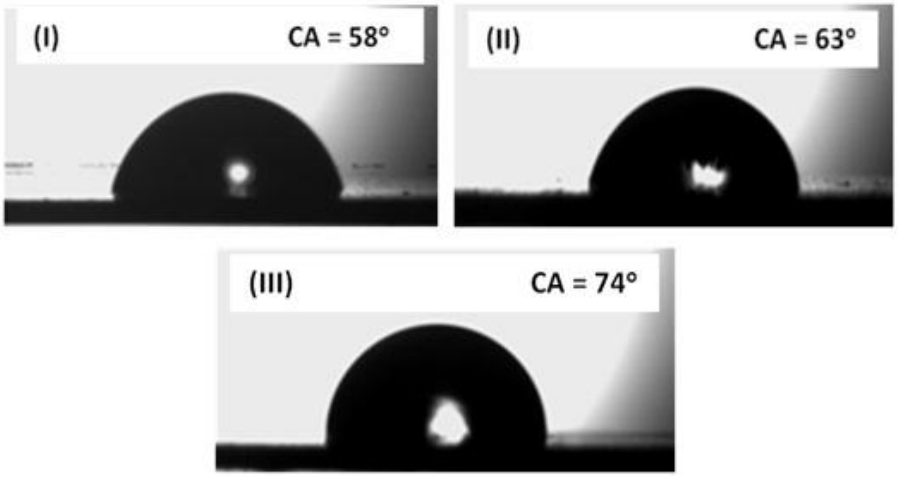

Fig. 5. Wettability of Ag_2Se thin films.
Sample (I) for bath concentration A, sample (II) for bath concentration B, sample (III) for bath concentration C.

3.7. FT-IR. The spontaneous orientations of dipole moments in semiconductors are carried out by infrared spectroscopy which gives information on atomic arrangement and inter atomic forces in the crystal lattice itself. The FT-IR spectra of Ag_2Se thin film is shown in Fig. 6. The FT-IR absorption bands were found at around wave numbers 1384.50 and 1633.67 cm^{-1} corresponding to the stretching vibrations of Ag – Se bond which confirms the Ag_2Se formation while the absorption around 3412 cm^{-1} is due to free –OH group as the samples were synthesized from aqueous electrolytic bath.

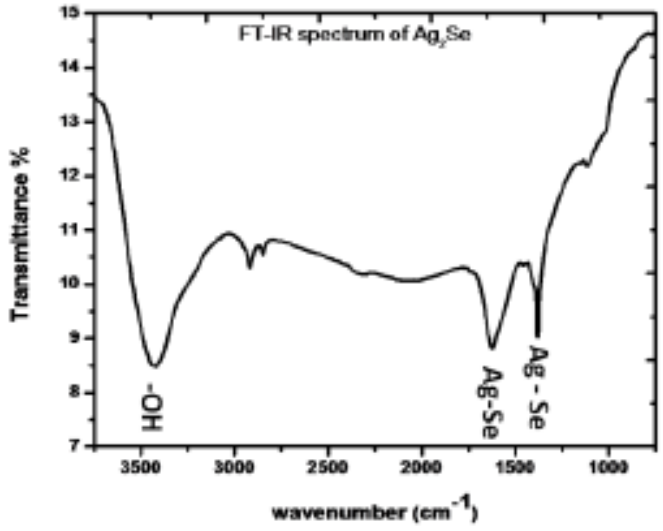

Fig. 6. FT-IR spectrum of Ag_2Se.

4. Holographic study

4.1. Double exposure holographic interferometry (DEHI). The double exposure holographic interferometry (DEHI) technique is used for thickness and stress measurement of Ag_2Se thin films for different bath concentrations. Figure 7 shows the experimental setup for recording hologram of the thin film.

time intervals. The holographic film was processed and replaced only in the reference wave path. The reconstructed image of substrate was observed with the reference beam, which shows the fringes localized on its surface [40, 41]. Using equations (7) – (9), estimated values of thickness, mass and stress of Ag_2Se thin film [38, 39, 42] are given in Table 3.

4.2. Variation in thickness and mass. Recorded holograms of Ag_2Se thin films by DEHI for bath concentration (A), (B) and (C) varying deposition time are shown in Fig. 8(a), Fig. 8(b) and Fig. 8(c) respectively. The increase in precursor concentration and deposition time increases the number of localized fringes with increase in thickness of thin film calculated using relation (7) shown in Fig. 9. These fringes are formed due to the interference between the light waves reflected from stainless steel substrate before and after deposition of Ag_2Se thin film. These fringes clearly indicate the deflection of stainless steel substrate due to the deposition of material onto it. Decrease in fringe width is observed with increase in both concentration and deposition time. The deposited mass of Ag_2Se in form of thin films increases with increase in concentration as well as deposition time as shown in Table 3.

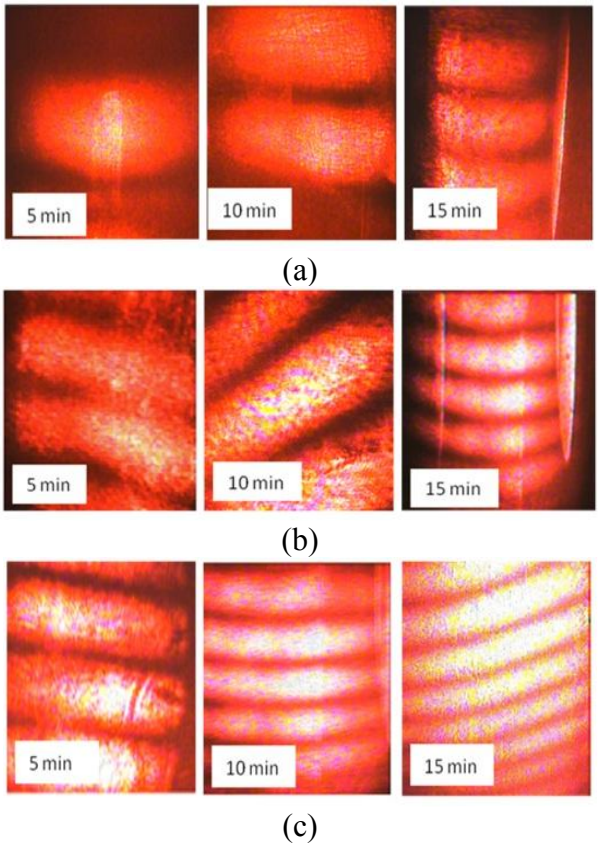

Fig. 8. Holograms of Ag_2Se thin films for bath concentration (a) - (A); (b) – (B); (c) – (C).

Thickness of thin film depends on applied voltage and concentration. Nucleation and growth of Ag_2Se in electrolyte increase with increase in concentration and time as well. As the concentration increases the number of cations and anions present in electrolyte accelerates the nucleation and growth processes resulting into higher thickness and more mass deposition for same time interval. Further increase in deposition time beyond 15 minutes, thickness goes on decreasing due to saturation and overgrowth of thin film with less adherence causing rapture and failure of thin film. Increase in the film thickness leads to agglomeration of Ag_2Se nano particles due to Van der Waals interaction between them causing increase in particle size and compactness of thin film revealed by XRD and microstructure respectively which decreases the wettability of Ag_2Se thin film.

Table 3. Holographic parameters for Ag_2Se thin films.

Bath Conc.	Deposition Time, min	No. of Fringes	Thickness, μm	Mass deposited, mg	Stress×10^9, dyne/cm^2
A	05	01	0.3164	0.779	2.66
	10	02	0.6328	1.560	1.33
	15	03	0.9492	2.399	0.889
B	05	02	0.6328	1.560	1.330
	10	03	0.9492	2.399	0.889
	15	05	1.582	3.899	0.533
C	05	03	0.9492	2.399	0.889
	10	05	1.582	3.899	0.533
	15	07	2.4148	5.460	0.380

5. Conclusions

Nanocrystalline Ag_2Se thin films have been successfully synthesized from aqueous precursor solution with simple eco- friendly electrodeposition technique at room temperature. Effects on crystallite size, band gap energy and wettability have been studied varying precursor concentration. The double exposure holographic interferometry (DEHI) technique has been successfully employed to explain the effect of concentration on physical properties of thin films by calculating thickness and stress of thin film. From the present study it is clear that nano crystalline silver selenide thin films will be grown at room temperature for various device applications.

Acknowledgment

Authors are very much grateful to UGC, New Delhi (India) for providing financial support through M.R.P. scheme no. F. No. 36-209/2008(SR).

References

[1] P.K. Khanna, B.K. Das // *Mater. Lett.* **58** (2004) 1030.
[2] P. Boolchand, W.J. Bresser // *Nature* **410** (2001) 1070.
[3] A. Nunez Rodriguez, M.T.S. Nair, P.K. Nair // *Semiconductor Science Technology* **20** (2005) 576.
[4] M. C. Santosh Kumar, B. Pradeep // *Bull. Mater. Sci.* **25** (2002) 407.
[5] M. Ferhat, J. Nagao // *Appl. Phys. Lett.* **88** (2000) 813.
[6] Z. Vucic, J. Gladic // *J. Cryst. Growth* **205** (1999) 136.
[7] M. Kobayashi // *Solid State Ionics* **39** (1990) *121.*
[8] B. Gates, Y. Wu, P. Yang, Y. Xia // *J. Am. Chem. Soc.* **123** (2001) 11500.
[9] M.M. Parish, P.B. Littlewood // *Nature* **426** (2003) 162.
[10] R. Xu, A. Husmann, T.F. Rosenbaum, M.L. Saboungi, J.E Enderby, P.B Littlewood // *Nature* **390** (1997) 57.
[11] Gur, N.A. Fromer, M.L. Geier, A.P. Alivisatos // *Science* **310** (2005) 462.
[12] V.L.Colvin, M.C. Schlamp, A.P. Alivisatos // *Nature* **370** (1994) 354.
[13] N. Tessler, V. Medvedev, M. Kazes, S. Kan, U. Banin // *Science* **295** (2002) 1506.
[14] D.L. Klein, R, Roth, A.K.L. Lim, A.P. Alivisatos, P.L. McEuen // *Nature* **389** (1997) 699.

[15] D.V. Talapin, C.B. Murray // *Science* **310** (2005) 86.
[16] W.C.W. Chan, S. Nie // *Science* **281** (1998) 2016.
[17] V. Damodara Das, D. Karunakaran // *J. Appl. Phys.* **68** (1990) 2105.
[18] C.D. Lokhande, K.M. Gadave // *Mater. Chem. Phys.* **36** (1993) 119.
[19] A.B. Kulkarni, M.D. Uplane, C.D. Lokhande // *Thin Solid Films* **260** (1995) 14.
[20] B. Pejova, M. Najdoski, I. Grozdanov, S.K. Dey // *Mater. Lett.* **43** (2000) 269.
[21] Y.J. Glanville, D.G. Narehood, P.E. Sokol, A. Amma, T. Mallouk // *J. Mater. Chem.* **12** (2002) 2433.
[22] S.J. Pawar, P.P. Chikode, V.J. Fulari, M.B. Dongare // *Mater. Sci. Eng. B* **37** (2007) 232.
[23] H. Cao, Y. Xiao, Y. Lu, J. Yin, B. Li, S. Wu, X. Wu // *Nano Res.* **3 (12)** (2010) 863.
[24] A. Sahu, L. Qi, M. S. Kang, D. Deng, D.J. Norris // *J. Am. Chem. Soc.* **133** (2011) 6509.
[25] P. T. Kissinger, W. R. Heineman // *J. of Chem. Edu. 60 (1983) 702.*
[26] S. Zhang, C. Fang, W. Wei, B. Jin, Y. Tian, Y. Shen, J. Yang, H. Gao // *J. Phys. Chem. C* **111** (2007) 4168.
[27] C. Ruizhi, X. Dongsheng, G. Guolin, T. Youqi // *J. of Mater. Chem.* **12** (2002) 1437.
[28] L.V. Azároff, R. Kaplow, N. Kato, R.J. Weiss, A.J.C. Wilson, R.A. Young, *X-ray Diffraction* (McGraw-Hill, New York, 1974).
[29] JCPDS card No. 24-1041
[30] B.D. Cullity, *Elements of X-rays Diffraction (*Addison-Wesley, London, 1978).
[31] C.M. Jiao; Z.Z. Wang, Z. Ye, Y. Hu, W.C. Fan // *J. Fire Sci.* **24** (2006) 47.
[32] D.T. Schoen, C. Xie, Y. Cui // *J. Am. Chem. Soc.* **129** (2007)
[33] H. Wang, L. Qi // *Adv. Funct. Mater.* **18** (2008) 1249.
[34] S.K. Batabyal, C. Basu, A.R. Das, G.S. Sanyal // *Crystal Growth & Design* **4** (2004) 509.
[35] F. Xia, H. Ge, Y. Hou, T. Sun, L. Chen, G. Zhang, L. Jiang // *Adv. Mater.* **19** (2007) 2520.
[36] R.S. Mane, H.Y. Hee, C.D. Lokhande, S.D. Sartale, S.H. Han // *Appl. Surf. Sci.* **246** (2005) 271.
[37] G.W. Stroke, *An introduction of coherent optics and holography* (Academic Press, New York, 1969).
[38] V.B. Prabhune, V.J. Fulari // *Opt. Commun.* **282** (2009) 2118.
[39] V.J. Fulari, V.P. Malekar, S.A. Gangawane // *Progress in Electromagnetic Research C* **12** (2010) 53.
[40] I.A. Lyavshuk, A.M. Lyalikov // *Quantum electron.* **36** (2006)154.
[41] A.M. Lyalikov // *Opt. Spektr.* **93** (2002) 512.
[42] G.A. Korn, T.M. Korn, *Mathematical Handbook for Scientists and Engineers* (McGraw-Hill, New York, 1961).